

Preparation and Characterization of NiO/CeO₂-ZrO₂/WO₃ Catalyst for Ethylene Dimerization: Effect of CeO₂ Doping and WO₃ Modifying on Catalytic Activity

Jong Rack Sohn,* Jong Soo Han, Hae Won Kim,† and Young Il Pae‡

Department of Applied Chemistry, Engineering College, Kyungpook National University, Daegu 702-701, Korea

*E-mail: jrsohn@knu.ac.kr

†Department of Advanced Materials and Environment Engineering, Kyung Il University, Kyungsan 712-701, Korea

‡Department of Chemistry, University of Ulsan, Ulsan 680-749, Korea

Received January 10, 2005

A series of catalysts, NiO/CeO₂-ZrO₂/WO₃, for ethylene dimerization was prepared by the precipitation and impregnation methods. For NiO/CeO₂-ZrO₂/WO₃ sample, no diffraction line of nickel oxide was observed up to 40 wt%, indicating good dispersion of nickel oxide on the surface of catalyst. The hexagonal and monoclinic phases of WO₃ up to the calcination temperature of 500 °C were observed, whereas the hexagonal phase of WO₃ completely was transformed into monoclinic phase of WO₃ at 600 °C and above. The role of CeO₂ in the catalysts was to form a thermally stable solid solution with zirconia and consequently to give high surface area and acidity. The catalytic activities for ethylene dimerization were correlated with the acidity of catalysts measured by the ammonia chemisorption method. 25-NiO/5-CeO₂-ZrO₂/15-WO₃ containing 25 wt% NiO, 15 wt% WO₃ and 5 mol% CeO₂, and calcined at 400 °C exhibited a maximum catalytic activity due to the effects of WO₃ modifying and CeO₂ doping.

Key Words : Ethylene dimerization, NiO/CeO₂-ZrO₂/WO₃, Effect of CeO₂ doping, Characterization

Introduction

Heterogeneous catalysts for the dimerization and oligomerization of olefins, consisting mainly of nickel compounds supported on oxides, have been known for many years. A considerable number of papers have dealt with the problem of nickel-containing catalysts for ethylene dimerization.¹⁻¹² One of the remarkable features of this catalyst system is its activity in relation to a series of n-olefins. In contrast to usual acid-type catalysts, nickel oxide on silica or silica-alumina shows a higher activity for a lower olefin dimerization, particularly for ethylene.^{1-6,11} It has been reported that the dimerization activities of such catalysts are related to the acidic property of surface and low valent nickel ions. In fact, nickel oxide, which is active for C₂H₄-C₂D₄ equilibration, acquires an activity for ethylene dimerization upon addition of nickel sulfate, which is known to be an acid.¹³ A transition metal can also be supported on zeolite in the state of a cation or a finely dispersed metal. Several papers have treated ethylene dimerization on transition-metal cation exchanged zeolites.¹⁴⁻¹⁶

In the previous papers from this laboratory, it has been shown that NiO-TiO₂ and NiO-ZrO₂ modified with sulfate or tungstate ions are very active for ethylene dimerization.^{6,17-19} High catalytic activities in the reactions were attributed to the enhanced acidic properties of the modified catalysts, which originated from the inductive effect of S=O or W=O bonds of the complex formed by the interaction of oxides with sulfate or tungstate ions. Zirconium oxide, ZrO₂ is a very interesting material because of its thermal stability, its mechanical properties, and its basic, acidic, reducing, and oxidizing properties.²⁰ The potential for a heterogeneous

catalyst has yielded many papers on the catalytic activity of sulfated zirconia materials.²¹⁻²⁴ Sulfated zirconia incorporating Fe and Mn has been shown to be highly active for butane isomerization, catalyzing the reaction even at room temperature.²⁵ However, it is known that for zirconia-supported catalyst its surface area and catalytic activity are decreasing under the severe reaction condition such as high temperature above 600 °C. As an extension of our study on ethylene dimerization, in this paper we report a new solid catalyst prepared by doping ZrO₂ with CeO₂ and modifying with WO₃ to improve catalytic activity for ethylene dimerization and thermal stability.

Experimental Section

Catalysts. The CeO₂-ZrO₂ mixed oxide was prepared by a coprecipitation method using an aqueous ammonia as the precipitation reagent. The coprecipitate of Ce(OH)₃-Zr(OH)₄ was obtained by adding aqueous ammonia slowly into a mixed aqueous solution of cerium nitrate and zirconium oxychloride [Junsei Chemical Co.] at 25 °C with stirring until the pH of mother liquor reached about 8. NiO/CeO₂-ZrO₂ was prepared by adding aqueous ammonia slowly into a mixed solution of NiCl₂ solution and CeO₂-ZrO₂ with stirring until the pH of solution reached about 8.

The catalysts containing various tungsten oxide contents were prepared by adding an aqueous solution of ammonium metatungstate[(NH₄)₆(H₂W₁₂O₄₀)-nH₂O] to the NiO/CeO₂-ZrO₂ powder followed by drying and calcining at high temperatures for 1.5 h in air. This series of catalysts are denoted by their weight percentage of NiO and WO₃. For example, 25-NiO/5-CeO₂-ZrO₂/15-WO₃ indicates the catalyst

containing 25 wt% NiO, and 15 wt% WO₃, and containing 5 mol% CeO₂ regarding only ZrO₂.

Procedure. The catalytic activity for ethylene dimerization was determined at 20 °C using a conventional static system following pressure change from an initial pressure of 290 Torr. A fresh catalyst sample of 0.2 g was used for every run and the catalytic activity was calculated as the mol number of ethylene consumed in the initial 10 min. Reaction products were analyzed by gas chromatograph with a VZ-7 column at room temperature.

Chemisorption of ammonia was employed as a measure of acid amount of catalysts. The amount of chemisorption was obtained as the irreversible adsorption of ammonia.²⁶⁻²⁸ The specific surface area was determined by applying the BET method to the adsorption of nitrogen at -196 °C.

FTIR (Fourier transform infrared) spectra were obtained in a heatable gas cell at room temperature using a Mattson Model GL6030E spectrometer. Self-supporting catalyst wafers contained about 9 mg/cm². Prior to obtaining the spectra, the samples were heated under vacuum at 500 °C for 1 h.

X-ray photoelectron spectra was obtained with a VG scientific model ESCALAB MK-11 spectrometer. Al K_α and Mg K_α were used as the excitation source, usually at 12 kV, 20 mA. The analysis chamber was at 10⁻⁹ torr or better and the spectra of sample, as fine powder, were analyzed. Binding energies were referenced to the C_{1s} level of the adventitious carbon at 285.0 eV.

Catalysts were checked in order to determine the structure of the support as well as that of tungsten oxide by means of a Jeol Model JDX-8030 diffractometer, employing CuK_α (Ni-filtered) radiation.

DSC measurements were performed by a PL-STA model 1500H apparatus in air, and the heating rate was 5 °C per minute. For each experiment 10-15 mg of sample was used.

Results and Discussion

Crystalline Structures of NiO/CeO₂-ZrO₂/WO₃. The crystalline structures of 25-NiO/5-CeO₂-ZrO₂/15-WO₃ calcined in air at different temperatures for 1.5 h were examined. As shown in Figure 1, the catalyst was amorphous to X-ray diffraction up to 300 °C. However, for the calcination temperature of 400 °C XRD data indicated a three-phase mixture of hexagonal and monoclinic phases of WO₃ and tetragonal phase of ZrO₂. The amount of tetragonal phase of ZrO₂ increased with increasing calcination temperature, indicating that the interaction between NiO or WO₃ and ZrO₂ hinders the transition of ZrO₂ from amorphous to tetragonal phase.^{29,30} The presence of NiO and WO₃ strongly influences the development of textural properties with temperature in comparison with pure ZrO₂. In fact, it is reported that for pure ZrO₂ two phases of tetragonal and monoclinic ZrO₂ are present at the calcination temperature of 350 °C because of no interaction of zirconia.³¹ As shown in Figure 1, the hexagonal phase of WO₃ completely was transformed into the monoclinic phase of WO₃ at 600 °C. No phase of NiO was observed in any phase at all

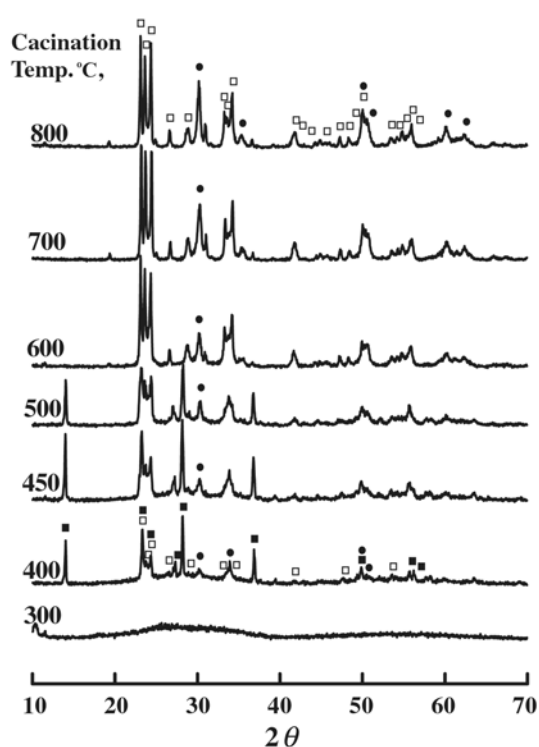


Figure 1. X-ray diffraction patterns of 25-NiO/5-CeO₂-ZrO₂/15-WO₃ as a function of calcination temperature: ■, hexagonal phase of WO₃; □, monoclinic phase of WO₃; ●, tetragonal phase of ZrO₂.

calcination temperature, indicating good dispersion of NiO on the surface of ZrO₂ support due to the interaction between them.

XRD patterns of 25-NiO/5-CeO₂-ZrO₂/WO₃ calcined at 400 °C for 1.5 hr as a function of WO₃ content are shown in Figure 2. WO₃ was amorphous to X-ray diffraction up to 5 wt%, indicating good dispersion on the surface of catalyst. However, from 10 wt% WO₃ XRD data indicated a three-phase mixture of hexagonal and monoclinic phases of WO₃ and tetragonal phase of ZrO₂. For the calcination temperature of 400 °C the hexagonal phase of WO₃ was predominantly present in comparison with the monoclinic phase of WO₃.

XRD patterns of NiO/5-CeO₂-ZrO₂/15-WO₃ calcined at 400 °C for 1.5 hr as a function of NiO content are shown in Figure 3. NiO was amorphous to X-ray diffraction regardless of NiO content up to 40 wt% NiO, indicating excellent dispersion on the surface of catalyst. However, the other components, WO₃ and ZrO₂ except NiO were observed as crystalline forms at 10 wt% WO₃ and above. Namely, hexagonal and monoclinic phases of WO₃ and tetragonal phase of ZrO₂ were appeared in the range of 15-40 wt% NiO.

XRD patterns of 25-NiO/5-CeO₂-ZrO₂/WO₃ calcined at 700 °C for 1.5 hr as a function of WO₃ content are shown in Figure 4. Unlike the 25-NiO/5-CeO₂-ZrO₂/WO₃ calcined at 400 °C, in the case of samples calcined at 700 °C only monoclinic phase of WO₃ without hexagonal phase of WO₃ was observed and the amount increased with increasing

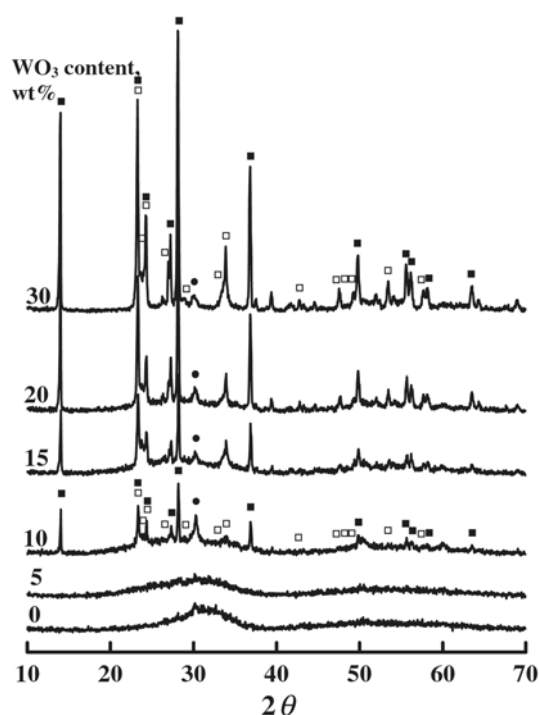


Figure 2. X-ray diffraction patterns of 25-NiO/5-CeO₂-ZrO₂/WO₃ calcined at 400 °C for 1.5 hr as a function of WO₃ content: ■, hexagonal phase of WO₃; □, monoclinic phase of WO₃; ●, tetragonal phase of ZrO₂.

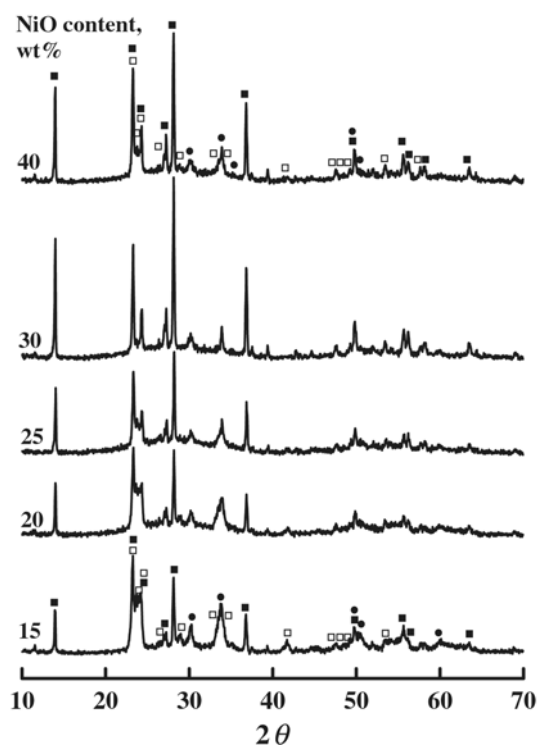


Figure 3. X-ray diffraction patterns of NiO/5-CeO₂-ZrO₂/15-WO₃ calcined at 400 °C for 1.5 hr as a function of NiO content: ■, hexagonal phase of WO₃; □, monoclinic phase of WO₃; ●, tetragonal phase of ZrO₂.

WO₃ content, because all hexagonal phase of WO₃ was transformed into monoclinic phase at high calcination

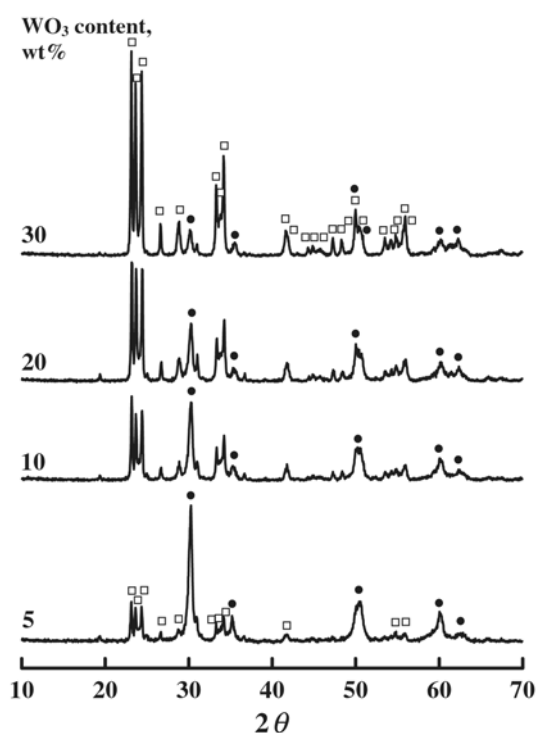


Figure 4. X-ray diffraction patterns of 25-NiO/5-CeO₂-ZrO₂/WO₃ calcined at 700 °C for 1.5 hr as a function of WO₃: ■, hexagonal phase of WO₃; □, monoclinic phase of WO₃; ●, tetragonal phase of ZrO₂.

temperature of 700 °C. For the ZrO₂ only tetragonal phase of ZrO₂ was observed and the amount decreased with increasing WO₃ content because of the decrease of relative amount of ZrO₂ regarding all components.

X-ray Photoelectron Spectra. Interactions with a support can dramatically change the properties metals or metal oxides.³² Figure 5 shows the W 4f spectra of some 25-NiO/5-CeO₂-ZrO₂/WO₃ samples containing different tungsten oxide contents and calcined at 500 °C. The W 4f_{7/2} binding energy measured for 25-NiO/5-CeO₂-ZrO₂/WO₃ samples occurred at 36 eV and corresponds to tungsten in the +6 oxidation state (WO₃).³³ Generally, the spectrum of supported WO₃ is broader than that of WO₃ due to the interaction between the WO₃ and support. It is known that there is a very strong interaction between WO₃ and Al₂O₃ so that tungsten oxide species is present as W⁺⁶ after calcination of WO₃/Al₂O₃ sample. As shown in Figure 5, for 25-NiO/5-CeO₂-ZrO₂/WO₃ samples calcined in air tungsten oxide species are present as W⁺⁶, indicating the strong interaction between WO₃ and CeO₂-ZrO₂. For 25-NiO/5-CeO₂-ZrO₂/30-WO₃, it seems likely that above monolayer coverage crystalline WO₃ exists on the surface of 5-CeO₂-ZrO₂ and well can be reduced to metallic W during calcination.³⁴

Infrared Spectra. To examine the structure of tungsten oxide complex under dehydration conditions, IR spectra of 25-NiO/5-CeO₂-ZrO₂/WO₃ samples were obtained in a heatable gas cell after evacuation at 500 °C for 1 h. The in situ IR spectra for 25-NiO/5-CeO₂-ZrO₂/WO₃ having different WO₃ contents are presented for the range 1100-900 cm⁻¹

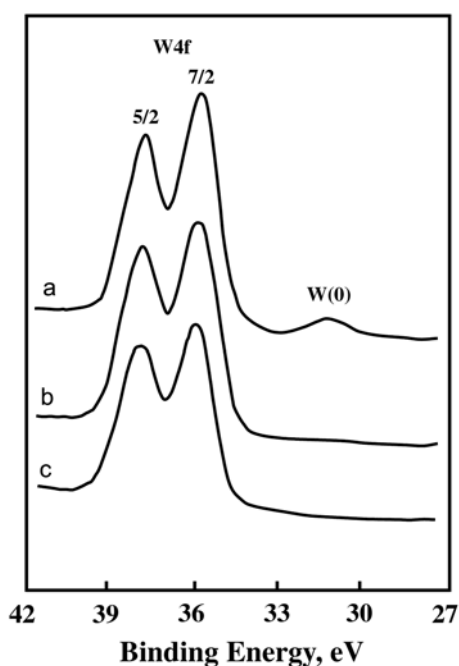


Figure 5. W_{4f} XPS of (a) 25-NiO/5-CeO₂-ZrO₂/30-WO₃, (b) 25-NiO/5-CeO₂-ZrO₂/15-WO₃, and (c) 25-NiO/5-CeO₂-ZrO₂/10-WO₃.

in Figure 6. The infrared single band at 1012 cm⁻¹ is due to the symmetrical W=O stretching mode of the tungsten oxide complex coordinated to the 5-CeO₂-ZrO₂ surface. The same results have been obtained at the other samples. This shows that the dehydration changes the molecular structures and that the two-dimensional tetrahedrally coordinated tungsten oxide species as well as the octahedrally coordinated

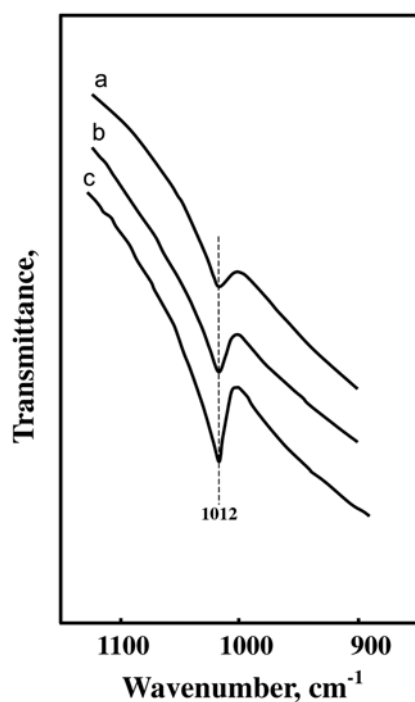


Figure 6. Infrared spectra of (a) 25-NiO/5-CeO₂-ZrO₂/5-WO₃, (b) 25-NiO/5-CeO₂-ZrO₂/10-WO₃, and (c) 25-NiO/5-CeO₂-ZrO₂/15-WO₃ evacuated at 500 °C for 1.5 hr.

polytungstate species are converted into the same highly distorted octahedrally coordinated structure as proposed for the WO₃/TiO₂ system by Wachs *et al.*³⁴ For the 25-NiO/5-CeO₂-ZrO₂/WO₃ samples evacuated at 500 °C, as shown in Figure 6, the band intensity at 1012 cm⁻¹ increases with increasing the WO₃ content, indicating that the higher the WO₃ content, the more the octahedrally coordinated WO₃ species.

Thermal Analysis. In X-ray diffraction pattern, it was shown that the structure of catalysts was different depending on the calcined temperature. To examine the thermal properties for the precursors of samples more clearly, their thermal analysis has been carried out and the results are illustrated in Figure 7. For pure ZrO₂ the DSC curve showed a broad endothermic peak below 200 °C due to water elimination, and a sharp exothermic peaks at 418 °C due to the phase transition of ZrO₂ from amorphous to tetragonal.³⁵ In the case of NiO/5-CeO₂-ZrO₂ a broad endothermic peak appeared below 200 °C is also due to the water elimination. However, it is of interest to see the influence of NiO on the crystallization of ZrO₂ from amorphous to tetragonal phase. As shown in Figure 7, the exothermic peak due to the phase transition of ZrO₂ appeared at 418 °C for pure ZrO₂, while for NiO/5-CeO₂-ZrO₂ it was shifted to higher temperatures, 421-514 °C. It is considered that the interaction between NiO and ZrO₂ delays the transition of ZrO₂ from amorphous to tetragonal phase.^{29,30} These results are in good agreement with those of X-ray diffraction described above. No crystalline phase of NiO was observed in X-ray diffraction patterns due to the interaction between NiO and ZrO₂.

Surface Properties of Catalysts. It is necessary to examine the effect of WO₃, NiO, and CeO₂ on the surface properties of catalysts, that is, specific surface area, acidity,

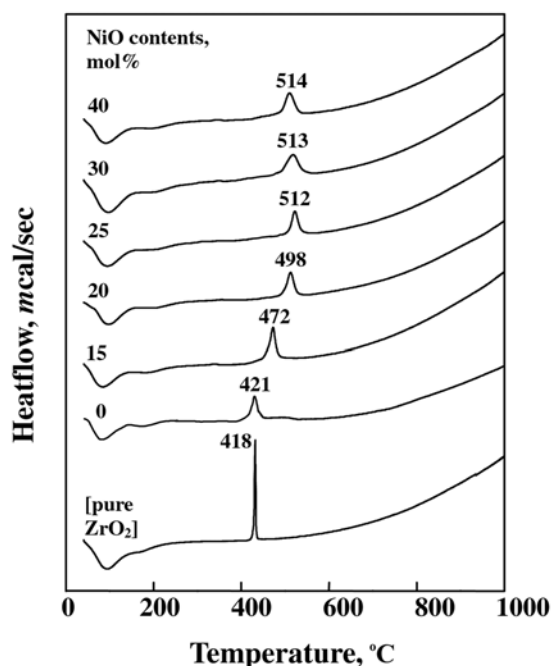


Figure 7. DSC curves of NiO/5-CeO₂-ZrO₂ precursors having different NiO contents.

and acid strength. The specific surface area and acidity of 25-NiO/5-CeO₂-ZrO₂/WO₃ having different WO₃ contents and calcined at 400 °C for 1.5 h are listed in Table 1. The presence of tungsten oxide influences the surface area and acidity in comparison with the sample without WO₃. The specific surface area and acidity increase gradually with increasing tungsten oxide content up to 15 wt% of WO₃. It seems likely that the interaction between tungsten oxide and ZrO₂ not only protects catalysts from sintering, but increase the acidity and acid strength due to the double bond nature of the W=O described below.

In addition to tungsten oxide content, we examined the effect of NiO on the surface area and acidity values. The surface area and acidity of NiO/5-CeO₂-ZrO₂/15-WO₃ having different NiO contents and calcined at 400 °C for 1.5 h are listed in Table 2. Similarly to WO₃, NiO also influenced both surface area and acidity values, indicating that the addition of NiO increased gradually both surface area and acidity with increasing NiO content up to 25 wt%. It is known that thermal resistance of zirconia against sintering can be considerably improved by incorporation a second oxide.^{36,37}

More active and stable catalyst can be obtained by addition of transition metal, especially noble metals.³⁸⁻⁴⁰ Recently, we reported that the role of Ce in CeO₂-ZrO₂ catalysts is to form a thermally stable solid solution with ZrO₂ and consequently to give high surface area.⁴¹ As listed in Table 3, the addition of CeO₂ to ZrO₂ also increase both surface area and acidity up to 5 mol% of CeO₂. Based on the results of XRD, all CeO₂ formed a solid solution with ZrO₂.

The acid strength of the catalysts was examined by a color change method, using Hammett indicator^{30,36} in sulphuryl chloride. 5-NiO/5-CeO₂-ZrO₂/15-WO₃ sample after evacuation at 500 °C for 1 h was estimated to have H₀ ≤ -14.5, indicating the formation of superacidic sites. Since it was

Table 1. Specific surface area and acidity of 25-NiO/5-CeO₂-ZrO₂/WO₃ containing different WO₃ contents and calcined at 400 °C for 1.5 hr

WO ₃ content (wt%)	Surface Area (m ² /g)	Acidity (μmol/g)
0	51	31
5	48	56
10	52	62
15	60	66
20	53	62
30	31	41

Table 2. Specific surface area and acidity of NiO/5-CeO₂-ZrO₂/15-WO₃ containing different NiO contents and calcined at 400 °C for 1.5 hr

NiO content (wt%)	Surface area (m ² /g)	Acidity (μmol/g)
15	42	55
20	52	63
25	60	66
30	39	51
40	31	42

Table 3. Specific surface area and acidity of 25-NiO/CeO₂-ZrO₂/15-WO₃ containing different CeO₂ contents and calcined at 400 °C for 1.5 hr

CeO ₂ content (mol%)	Surface area (m ² /g)	Acidity (μmol/g)
1	31	42
3	45	61
5	60	66
8	58	44
10	41	28

very difficult to observe the color of indicators adsorbed on the catalyst of high nickel oxide content, the low percentage of nickel oxide (5 wt %) was used in this experiment. Acids stronger than H₀ ≤ -11.93, which corresponds to the acid strength of 100% H₂SO₄, are superacids.²¹⁻²³ Consequently, NiO/CeO₂-ZrO₂/WO₃ catalysts would be solid superacids. The superacidic property is attributed to the double bond nature of the W=O in the complex formed by the interaction of ZrO₂ with tungstate, in analogy with the case of ZrO₂ modified with chromate and sulfate ion.^{36,42,43}

Infrared spectroscopic studies of ammonia adsorbed on solid surfaces have made it possible to distinguish between Brønsted and Lewis acid sites.⁴⁴⁻⁴⁶ Figure 8 shows the IR spectra of ammonia adsorbed on 25-NiO/5-CeO₂-ZrO₂/15-WO₃ sample evacuated at 400 °C for 1 hr. The band at 1445 is the characteristic peak of ammonium ion, which is formed on the Brønsted acid sites and the absorption peak at 1615 cm⁻¹ is contributed by ammonia coordinately bonded to Lewis acid sites,⁴⁴⁻⁴⁶ indicating the presence of both Brønsted and Lewis acid sites on the surface of 25-NiO/5-CeO₂-

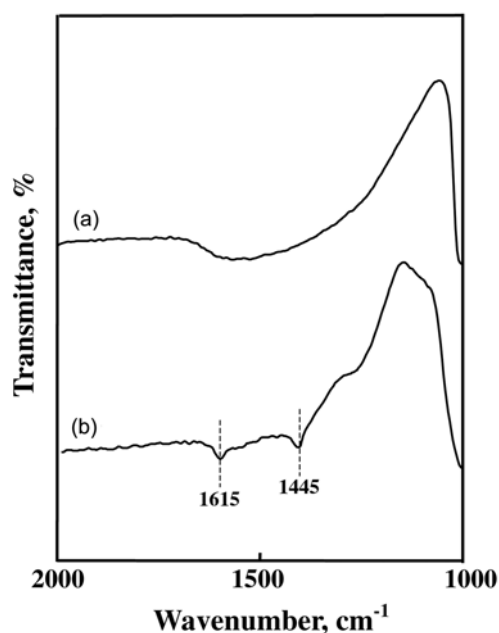


Figure 8. Infrared spectra of NH₃ adsorbed on 25-NiO/5-CeO₂-ZrO₂/15WO₃: (a) background of 25-NiO/5-CeO₂-ZrO₂/15-WO₃ after evacuation at 500 °C for 1 hr, (b) NH₃ adsorbed on (a), where gas was evacuated at 230 °C for 1 h.

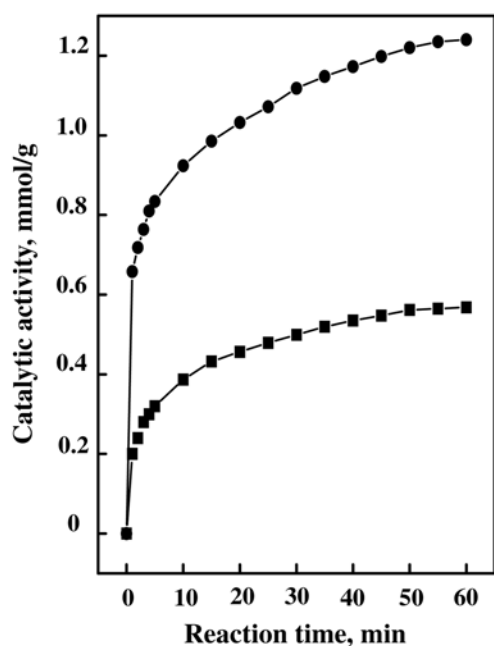


Figure 9. Time-course of ethylene dimerization over catalysts evacuated at 400 °C for 1.5 hr: ●, 25-NiO/5-CeO₂-ZrO₂/15-WO₃; ■, 25-NiO/1-CeO₂-ZrO₂/15-WO₃.

ZrO₂/15-WO₃ sample. Other samples having different WO₃ and NiO contents also showed the presence of both Lewis and Brönsted acids.

Ethylene Dimerization over NiO/CeO₂-ZrO₂/WO₃. NiO/CeO₂-ZrO₂/WO₃ catalysts were tested for their effectiveness in ethylene dimerization. It was found that over 25-NiO/5-CeO₂-ZrO₂/15-WO₃ and 25-NiO/1-CeO₂-ZrO₂/15-WO₃, ethylene was continuously consumed, as shown by the results presented in Figure 9, where catalysts were evacuated at 400 °C for 1.5 hr. Over NiO/CeO₂-ZrO₂/WO₃, ethylene was selectively dimerized to n-butenes. In the composition of n-butenes analyzed by gas chromatography, 1-butene was found to predominate exclusively at the initial reaction time, as compared with cis-butene and trans-butene. However, the amount of 1-butene decreases with the reaction time, while the amount of 2-butene increases. Therefore, it seems likely that the initially produced 1-butene is also isomerized to 2-butene during the reaction time.^{17,46} NiO/CeO₂-ZrO₂/WO₃ was very effective for ethylene dimerization, but NiO/CeO₂-ZrO₂ without WO₃ did not absolutely exhibit catalytic activity because the sample without WO₃ does not possess considerable acidity and acid strength enough to catalyze ethylene dimerization.

The catalytic activities of 25-NiO/5-CeO₂-ZrO₂/15-WO₃ were tested as a function of calcination temperature. The activities increased with the calcination temperature, reaching a maximum at 400 °C, after which the activities decreased. The decrease of catalytic activity after calcination above 400 °C seems to be due to the decrease of surface area and acidity at high calcination temperatures. In fact, the surface area of 25-NiO/5-CeO₂-ZrO₂/15-WO₃ calcined at 400 °C was found to be 60 m²/g, but that of sample calcined

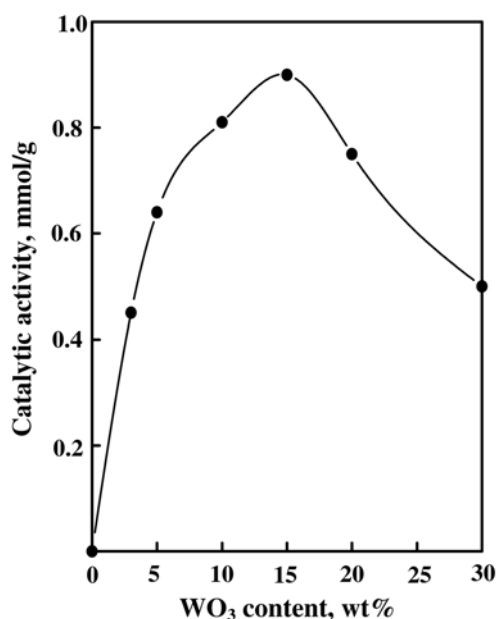


Figure 10. Catalytic activity of 25-NiO/5-CeO₂-ZrO₂/WO₃ for ethylene dimerization as a function of WO₃ content.

at 600 °C decreased to 28 m²/g. The acidity of the sample calcined at 400 and 600 °C was found to be 66 and 32 μmol/g, respectively.

Effect of WO₃ Modifying on Catalytic Activity. Recently, it has been reported that metal oxide modified with WO₃ can be used as an alternative catalyst in reactions requiring strong acid sites.²³ Several advantages of tungstate, over sulfate, as dopant include that it does not suffer from dopant loss during thermal treatment and it undergoes significantly less deactivation during catalytic reaction.

The effect of WO₃ content on the catalytic activity of 25-NiO/5-CeO₂-ZrO₂/WO₃ was examined, where the catalysts were evacuated at 400 °C for 1 hr. As shown in Figure 10, the maximum activity is obtained with the catalyst of 15 wt% WO₃. It is known that the active sites responsible for dimerization consist of a low-valent nickel and an acid.^{17,31,46} Therefore, it seems likely that the highest activity of catalyst containing 15 wt% WO₃ is related to its acidity and acid strength. The high acid strength and high acidity is responsible for the W=O bond nature of complex formed by the interaction between WO₃ and ZrO₂.^{23,47} As listed in Table 1, the acidity of 25-NiO/5-CeO₂-ZrO₂/15-WO₃ is the most among the catalysts. Of course, the acidity of catalysts is related to their specific surface area, as mentioned above. In fact, Table 1 shows that the specific surface area attained a maximum when the WO₃ content in 25-NiO/5-CeO₂-ZrO₂/WO₃ is 15 wt%. Although the sample without WO₃ was inactive as catalyst for ethylene dimerization, as shown in Figure 10, the 25-NiO/5-CeO₂-ZrO₂/WO₃ with WO₃ exhibited high catalytic activity even at room temperature.

Effect of NiO Content on Catalytic Activity. As mentioned above, the active site responsible for dimerization is suggested to consist of a low valent nickel ion and as acid, as observed in the nickel-containing catalyst.^{17,31,46} The term

'low valent nickel' originated from the fact that the NiO-SiO₂ catalyst was drastically poisoned by carbon monoxide, since a low valent nickel is favorable to chemisorbed carbon monoxide.⁴⁸ Kazansky concluded that Ni⁺ ions in NiCa-Y zeolite are responsible for the catalytic activity, using EPR spectroscopy to identify low valent nickel species.¹⁵ Therefore, nickel species is necessary to be active for ethylene dimerization. In fact, CeO₂-ZrO₂/WO₃ without NiO is inactive for ethylene dimerization.

The catalytic activity of NiO/5-CeO₂-ZrO₂/15-WO₃ containing different NiO contents were examined; the results are shown as a function of NiO content in Figure 11. Catalysts were evacuated at 400 °C for 1 hr before each reaction. The catalytic activity increased with increasing the NiO content, reaching a maximum at 25 wt%. Considering the experimental results of Table 2 and Figure 11, we think that the catalytic activities for ethylene dimerization are closely related to the change of surface area and the acidity of catalysts. For NiO/5-CeO₂-ZrO₂/15-WO₃ both catalytic activity and acidity reached maxima at 25 wt% of NiO. Good correlations have been found in many cases between the acidity and the catalytic activities for ethylene dimerization.^{4,42,46}

Effect of CeO₂ Doping on Catalytic Activity. The catalytic activity of 25-NiO/CeO₂-ZrO₂/15-WO₃ as a function of CeO₂ content for the reaction of ethylene dimerization was examined and the results are shown in Figure 12. The catalytic activity increased with increasing the CeO₂ content, reaching a maximum at 5 mol%. Considering the experimental results of Table 3 and Figure 12, the catalytic activities are also related to the changes of surface area and the acidity of catalysts. It was reported that a small amount of rare-earth elements in zirconia powder can stabilize the tetragonal and cubic phases over a wide range of temper-

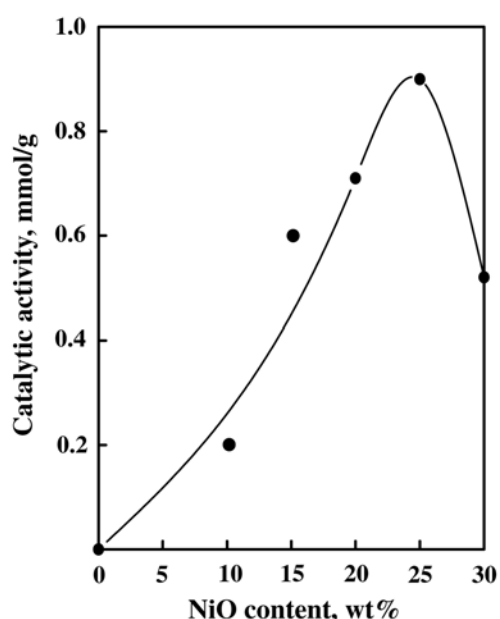


Figure 11. Catalytic activity of NiO/5-CeO₂-ZrO₂/15-WO₃ for ethylene dimerization as a function of NiO content.

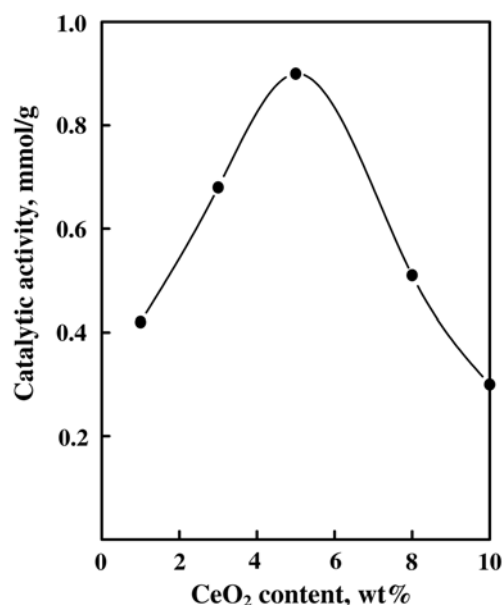


Figure 12. Catalytic activity of 25-NiO/CeO₂-ZrO₂/WO₃ for ethylene dimerization as a function of CeO₂ content.

ature.⁴⁹ This high surface area of Ce-doped samples compared with undoped samples is due to the doping effect of CeO₂ which makes zirconia a stable tetragonal phase⁵⁰ as confirmed by XRD. The role of CeO₂ in the catalysts is to form a thermally stable solid solution^{41,50} with zirconia and consequently to give their high surface area and acidity.

Correlation between Catalytic Activity and Acidity. The catalytic activities of NiO/CeO₂-ZrO₂/WO₃ containing different NiO, CeO₂, and WO₃ contents were examined; the results are shown as a function of acidity in Figure 13, where catalysts were evacuated at 400 °C for 1 h before reaction. Figure 13 shows good correlation between the catalytic activity and the acidity. It is confirmed that the catalytic activity gives a maximum at 25 wt% NiO, 5 mol % CeO₂ and 15 wt% WO₃. This seems to be correlated to the specific surface area and to the acidity of catalysts. The acidity of NiO/CeO₂-ZrO₂/WO₃ calcined at 400 °C was determined by the amount of NH₃ irreversibly adsorbed at 230 °C.^{4,6,9,51} As listed in Tables 1 and 2, the BET surface area and acidity attained a maximum extent for the 25-NiO/5-CeO₂-ZrO₂/15-WO₃ catalyst. As shown in Figure 13, the higher the acidity, the higher the catalytic activity. In this way it is demonstrated that the catalytic activity of NiO/CeO₂-ZrO₂/WO₃ essentially runs parallel to the acidity. Good correlations have been found in many cases between the acidity and the catalytic activities of solid acids. For example, the rates of both the catalytic decomposition of cumene and polymerization of propylene over SiO₂-Al₂O₃ catalysts were found to increase with increasing acid amount at strength H₀ ≤ +3.3.⁵² It has been reported that the catalytic activity of nickel-containing catalysts in ethylene dimerization as well as in butene isomerization is closely correlated with the acidity of the catalyst.^{4,42,46}

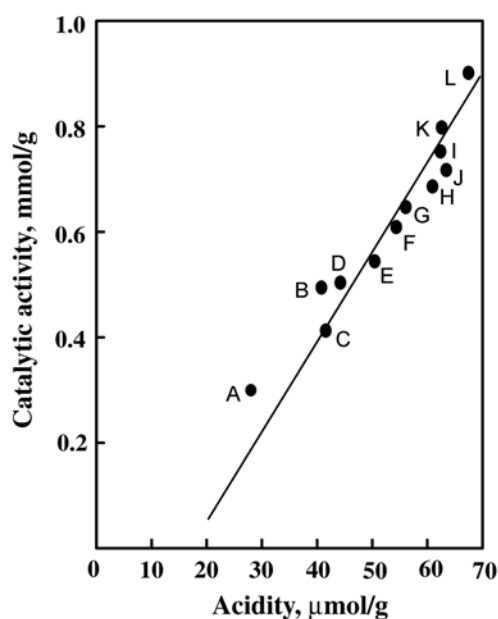


Figure 13. Correlation between catalytic activity of and acidity NiO/CeO₂-ZrO₂/WO₃ for ethylene dimerization: (A) 25-NiO/10-CeO₂-ZrO₂/15-WO₃; (B) 25-NiO/5-CeO₂-ZrO₂/30-WO₃; (C) 25-NiO/1-CeO₂-ZrO₂/15-WO₃; (D) 25-NiO/8-CeO₂-ZrO₂/15-WO₃; (E) 30-NiO/5-CeO₂-ZrO₂/15-WO₃; (F) 15-NiO/5-CeO₂-ZrO₂/15-WO₃; (G) 25-NiO/5-CeO₂-ZrO₂/5-WO₃; (H) 25-NiO/3-CeO₂-ZrO₂/15-WO₃; (I) 25-NiO/5-CeO₂-ZrO₂/20-WO₃; (J) 20-NiO/5-CeO₂-ZrO₂/15-WO₃; (K) 20-NiO/5-CeO₂-ZrO₂/10-WO₃; (L) 25-NiO/5-CeO₂-ZrO₂/15-WO₃.

Conclusions

For NiO/CeO₂-ZrO₂/WO₃ catalyst, no diffraction line of nickel oxide was observed up to 40 wt%, indicating good dispersion of nickel oxide on the surface of catalyst. The hexagonal and monoclinic phases of WO₃ up to the calcination temperature of 500 °C were observed, whereas the hexagonal phase of WO₃ completely was transformed into monoclinic phase of WO₃ at 600 °C and above. NiO/CeO₂-ZrO₂/WO₃ was very effective for ethylene dimerization, but CeO₂-ZrO₂/WO₃ without NiO or NiO/CeO₂-ZrO₂ without NiO does not absolutely exhibit catalytic activity. The high catalytic activity of NiO/CeO₂-ZrO₂/WO₃ was related to the increase of acidity and thermal stability due to the effects of WO₃ modifying and CeO₂ doping.

Acknowledgements. This work was supported by Korea Research Foundation Grant (KRF-2003-002-D00078). We wish to thank Korea Basic Science Institute (Daegu Branch) for the use of X-ray diffractometer.

References

- Urabe, K.; Koga, M.; Izumi, Y. *J. Chem. Soc., Chem. Commun.* **1989**, 807.
- Bernardi, F.; Bottoni, A.; Rossi, I. *J. Am. Chem. Soc.* **1998**, *120*, 7770.
- Sohn, J. R.; Ozaki, A. *J. Catal.* **1979**, *59*, 303.
- Sohn, J. R.; Ozaki, A. *J. Catal.* **1980**, *61*, 29.
- Wendt, G.; Fritsch, E.; Schöllner, R.; Siegel, H. Z. *Anorg. Allg. Chem.* **1980**, *467*, 51.
- Sohn, J. R.; Shin, D. C. *J. Catal.* **1996**, *160*, 314.
- Berndt, G. F.; Thomson, S. J.; Webb, G. J. *J. Chem. Soc. Faraday Trans. 1* **1983**, *79*, 195.
- Herwijnen, T. V.; Doesburg, H. V.; Jong, D. V. *J. Catal.* **1973**, *28*, 391.
- Sohn, J. R.; Park, W. C.; Kim, H. W. *J. Catal.* **2002**, *209*, 69.
- Sohn, J. R.; Park, W. C. *Bull. Korean Chem. Soc.* **2000**, *21*, 1063.
- Wendt, G.; Hentschel, D.; Finster, J.; Schöllner, R. *J. Chem. Soc. Faraday Trans. 1* **1983**, *79*, 2013.
- Kimura, K.; Ozaki, A. *J. Catal.* **1964**, *3*, 395.
- Maruya, K.; Ozaki, A. *Bull. Chem. Soc. Jpn.* **1973**, *46*, 351.
- Hartmann, M.; Pöppel, A.; Kevan, L. *J. Phys. Chem.* **1996**, *1009*, 906.
- Elev, I. V.; Shelimov, B. N.; Kazansky, V. B. *J. Catal.* **1984**, *89*, 470.
- Choo, H.; Kevan, L. *J. Phys. Chem. B* **2001**, *105*, 6353.
- Sohn, J. R.; Kim, H. J. *J. Catal.* **1986**, *101*, 428.
- Sohn, J. R.; Lee, S. Y. *Appl. Catal. A: Gen.* **1997**, *164*, 127.
- Sohn, J. R.; Kim, H. W.; Park, M. Y.; Park, E. H.; Kim, J. T.; Park, S. E. *Appl. Catal.* **1995**, *128*, 127.
- Comelli, R. A.; Vera, C. R.; Parera, J. M. *J. Catal.* **1995**, *151*, 96.
- Sohn, J. R. *J. Ind. Eng. Chem.* **2004**, *10*, 1.
- Tanabe, K.; Misono, M.; Ono, Y.; Hattori, H. *New Solid Acids and Bases*; Elsevier Science and Amsterdam: 1989; Chap. 4.
- Arata, K. *Adv. Catal.* **1990**, *165*, 37.
- Hino, M.; Kobayashi, S.; Arata, K. *J. Am. Chem. Soc.* **1979**, *101*, 6439.
- Cheung, T. K.; Gates, B. C. *J. Catal.* **1997**, *168*, 522.
- Sohn, J. R.; Lee, S. H.; Park, W. C.; Kim, H. W. *Bull. Korean Chem. Soc.* **2004**, *25*, 657.
- Sohn, J. R.; Seo, D. H.; Lee, S. H. *J. Ind. Eng. Chem.* **2004**, *10*, 309.
- Sohn, J. R.; Lee, S. H. *Appl. Catal. A: Gen.* **2004**, *266*, 89.
- Sohn, J. R.; Chun, E. W.; Pae, Y. I. *Bull. Korean Chem. Soc.* **2003**, *24*, 1785.
- Sohn, J. R.; Cho, S. G.; Pae, Y. I.; Hayashi, S. *J. Catal.* **1996**, *159*, 170.
- Sohn, J. R.; Park, W. C. *Appl. Catal. A: Gen.* **2002**, *11*, 230.
- Tauster, S. J.; Fung, S. C.; Baker, R. T. K.; Horsley, J. A. *Science* **1981**, *211*, 1121.
- Wachs, I. E.; Chersich, E. C.; Hardenbergh, J. H. *Appl. Catal.* **1985**, *13*, 335.
- Vuurman, M. A.; Wachs, I. E.; Hirt, A. M. *J. Phys. Chem.* **1991**, *95*, 9928.
- Sohn, J. R.; Kim, J. G.; Kwon, T. D.; Park, E. H. *Langmuir* **2002**, *18*, 1666.
- Sohn, J. R.; Ryu, S. G. *Langmuir* **1993**, *9*, 126.
- Mercera, P. D. L.; van Ommen, J. G.; Doesburg, E. B. M.; Burggraaf, A. J.; Ross, J. R. H. *Appl. Catal.* **1990**, *57*, 127.
- Ebitani, K.; Konishi, J.; Hattori, H. *J. Catal.* **1991**, *130*, 257.
- Adeeva, V.; Lei, G. D.; Sachtler, W. M. H. *Appl. Catal.* **1994**, *118*, L11-L15.
- Lin, C. H.; Hsu, C. Y. *J. Chem. Soc. Chem. Commun.* **1992**, 1479.
- Sohn, J. R.; Lim, J. S.; Lee, S. H. *Chem. Lett.* **2004**, *33*, 1490.
- Sohn, J. R.; Park, W. C.; Kim, H. W. *J. Catal.* **2002**, *209*, 69.
- Sohn, J. R.; Kim, H. W. *J. Mol. Catal.* **1989**, *52*, 361.
- Basila, M. R.; Kantner, T. R. *J. Phys. Chem.* **1967**, *71*, 467.
- Satsuma, A.; Hattori, A.; Mizutani, K.; Furuta, A.; Miyamoto, A.; Hattori, T.; Murakami, Y. *J. Phys. Chem.* **1988**, *92*, 6052.
- Sohn, J. R.; Park, W. C. *Appl. Catal. A: Gen.* **2003**, *239*, 269.
- Sohn, J. R.; Park, M. Y. *Langmuir* **1998**, *14*, 6140.
- Kimura, K.; A-I H.; Ozaki, A. *J. Catal.* **1990**, *18*, 271.
- Loong, C.-K.; Ozawa, M. *J. Alloys Compd.* **2000**, *60*, 303.
- Dong, W.-S.; Roh, H.-S.; Jun, K.-W.; Park, S.-E.; Oh, Y.-S. *Appl. Catal. A: Gen.* **2002**, *226*, 63.
- Pae, Y. I.; Bae, M. H.; Park, W. C.; Sohn, J. R. *Bull. Korean Chem. Soc.* **2004**, *25*, 1881.
- Tanabe, K. *Solid Acids and Bases*; Kodansha: Tokyo, 1970; p 103.